Adv Comput Math (2013) 38:63–82
DOI 10.1007/s10444-011-9226-z

An interpolation scheme for designing rational rotation-minimizing camera motions

Rida T. Farouki · Carlotta Giannelli · Alessandra Sestini

Received: 28 October 2010 / Accepted: 15 March 2011 /
Published online: 23 September 2011

Abstract When a moving (real or virtual) camera images a stationary object, the use of a *rotation-minimizing directed frame* (RMDF) to specify the camera orientation along its path yields the least apparent rotation of the image. The construction of such motions, using curves that possess rational RMDFs, is considered herein. In particular, the construction entails interpolation of initial/final camera positions and orientations, together with an initial motion direction. To achieve this, the camera path is described by a rational space curve that has a rational RMDF and interpolates the prescribed data. Numerical experiments are used to illustrate implementation of the method, and sufficient conditions on the two end frame orientations are derived, to ensure the existence of exactly one interpolant. By specifiying a sequence of discrete camera positions/orientations and an initial motion direction, the method can be used to construct general rotation-minimizing camera motions.

Communicated by Helmut Pottmann.

R. T. Farouki (✉)
Department of Mechanical and Aerospace Engineering, University of California,
Davis, CA 95616, USA
e-mail: farouki@ucdavis.edu

C. Giannelli
Dipartimento di Sistemi e Informatica, Università degli Studi di Firenze,
Viale Morgagni 65, 50134 Firenze, Italy
e-mail: giannelli@dsi.unifi.it

A. Sestini
Dipartimento di Matematica "Ulisse Dini", Università degli Studi di Firenze,
Viale Morgagni 67a, 50134 Firenze, Italy
e-mail: alessandra.sestini@unifi.it

Keywords Camera orientation · Directed frames · Rotation-minimizing frames · Angular velocity · Pythagorean curves · Quaternions · Interpolation

1 Introduction

A *directed* frame $(\mathbf{o}(t), \mathbf{u}(t), \mathbf{v}(t))$ along a space curve $\mathbf{r}(t)$ is an orthonormal basis for $\mathbb{R}^3$ such that $\mathbf{o}(t) = \mathbf{r}(t)/|\mathbf{r}(t)|$ is the unit *polar vector*, defining the direction from the origin to each curve point, while $\mathbf{u}(t)$, $\mathbf{v}(t)$ span the plane orthogonal to $\mathbf{o}(t)$—the *image plane* in camera orientation control. Such a frame is said to be *rotation-minimizing* if its angular velocity $\boldsymbol{\omega}(t)$ maintains a zero component along the polar vector $\mathbf{o}(t)$, i.e., $\mathbf{o}(t) \cdot \boldsymbol{\omega}(t) \equiv 0$. Rotation-minimizing directed frames (RMDFs) were introduced in [7], motivated by the problem of controlling the orientation of a (real or virtual) camera about its optical axis, as it traverses a curved path, so as to incur the least apparent rotation of the object (fixed at the origin) being imaged.[1]

Rotation-minimizing *adapted* frames (RMAFs) have received much more attention than *directed* frames. For an adapted frame on a space curve, one frame vector coincides with the curve tangent, while the other two span the curve normal plane—the frame is rotation-minimizing if its angular velocity maintains a zero component along the curve tangent. RMAFs are useful in robotics, animation, spatial motion control, geometrical sweeping operations, etc. In particular, the possibility of constructing exact *rational* RMAFs on polynomial space curves [1, 6, 9, 11] is a promising new development.

The focus of this paper is on the construction of rational space curves that have rational RMDFs, by interpolation of initial/final positions $\mathbf{p}_i = d_i\mathbf{o}_i$ and $\mathbf{p}_f = d_f\mathbf{o}_f$ (where $d_i, d_f > 0$) and directed frames $(\mathbf{o}_i, \mathbf{u}_i, \mathbf{v}_i)$ and $(\mathbf{o}_f, \mathbf{u}_f, \mathbf{v}_f)$. Now the theory of directed frames coincides [7] with that of adapted frames, applied to the *anti-hodograph*—i.e., indefinite integral—of the given curve. Correspondingly, polynomial curves with rational directed frames must be *Pythagorean* (P) curves [7], just as polynomial curves with rational adapted frames must be *Pythagorean-hodograph* (PH) curves [6, 9, 13]—since only P curves have rational unit polar vectors, and only PH curves have rational unit tangent vectors. These observations allow many results, established in the context of PH curves, to be carried over to P curves. In particular, the present study relies extensively on methods developed [10] in the context of motion interpolation using PH curves with rational RMAFs.

The Hermite interpolation algorithm for polynomial PH curves that have rational RMAFs [10] is adapted herein to formulate an analogous Lagrange interpolation algorithm for polynomial P curves that have rational RMDFs. The algorithm in [10] constructs spatial rigid-body motions, specified as G^1 PH quintic space curves with rational RMAFs. Its adaptation to the present context, however, yields spatial P quartics with rational RMDFs that are only

[1] This issue has not been addressed in prior camera motion studies—e.g., [4, 14].

G^0 continuous. To achieve a G^1 continuous scheme for rotation-minimizing camera motion, one might consider the full Hermite interpolation problem—i.e., interpolation of initial/final unit tangents $\mathbf{t}_i$, $\mathbf{t}_f$ for the path, as well as initial/final positions and directed frames.

To obtain sufficient degrees of freedom, however, this requires P curves of degree > 4. Now the condition for rational RMAFs on PH curves of degree n is equivalent to that for rational RMDFs on P curves of degree $n-1$. Although sufficient-and-necessary conditions for rational RMAFs are now available [11] for PH curves of arbitrary degree, only degree 5 PH curves (analogous to degree 4 P curves) have thus far been characterized [6, 9] by simple coefficient constraints, amenable to constructive algorithms.

As an alternative to constructing G^1 spatial motions, we consider "semi-G^1 motions," in which one of the two end-tangent interpolation constraints is relaxed, and we employ a rational (rather than polynomial) interpolant curve. The proposed scheme constructs a rational curve $\boldsymbol{\rho}(t)$ with a rational RMDF $(\mathbf{o}(t), \mathbf{u}(t), \mathbf{v}(t))$ for $t \in [0, 1]$, where $\mathbf{o}(t) = \boldsymbol{\rho}(t)/|\boldsymbol{\rho}(t)|$ is the unit polar vector, that satisfies the end-point interpolation conditions

$$\boldsymbol{\rho}(0) = d_i \mathbf{o}_i\,, \qquad (\mathbf{o}(0), \mathbf{u}(0), \mathbf{v}(0)) = (\mathbf{o}_i, \mathbf{u}_i, \mathbf{v}_i)\,, \qquad \frac{\boldsymbol{\rho}'(0)}{|\boldsymbol{\rho}'(0)|} = \mathbf{t}_i\,, \tag{1}$$

$$\boldsymbol{\rho}(1) = d_f \mathbf{o}_f\,, \qquad (\mathbf{o}(1), \mathbf{u}(1), \mathbf{v}(1)) = (\mathbf{o}_f, \mathbf{u}_f, \mathbf{v}_f)\,, \tag{2}$$

where we assume that $\mathbf{o}_f \neq \mathbf{o}_i$. It is convenient to decompose $\mathbf{t}_i$ in the form

$$\mathbf{t}_i = c_i \mathbf{f}_i + s_i \mathbf{o}_i\,, \tag{3}$$

where $\mathbf{f}_i \cdot \mathbf{o}_i = 0$, $|\mathbf{f}_i| = 1$, $c_i^2 + s_i^2 = 1$, and $c_i > 0$.

The plan for this paper is as follows. After presenting an overall outline of the scheme in Section 2, the basic definitions and properties of polynomial Pythagorean curves that possess rational RMDFs are reviewed in Section 3. Section 4 then discusses construction of a quartic P curve $\mathbf{r}(t)$ with rational RMDF that interpolates the given end frames, in terms of which the rational polar indicatrix $\mathbf{o}(t) = \mathbf{r}(t)/|\mathbf{r}(t)|$ is determined in Section 5. The interpolant $\boldsymbol{\rho}(t) = \rho(t)\,\mathbf{o}(t)$ is defined in Section 6 by scaling $\mathbf{o}(t)$ with a polynomial $\rho(t)$ so as to interpolate the given end points and initial motion direction. Finally, Section 7 outlines the algorithm for constructing camera motion interpolants, Section 8 presents some computed examples, and Section 9 summarizes the key results of this paper and suggests topics for further study. The Appendix contains some rather technical results that are used in the body of the paper.

2 General procedure

For a space curve satisfying $\mathbf{r}(t) \neq \mathbf{0}$ for $t \in [0, 1]$ the polar vector $\mathbf{o}(t) = \mathbf{r}(t)/|\mathbf{r}(t)|$ defines a curve on the unit sphere—the *polar indicatrix* of $\mathbf{r}(t)$. Now the variation of the RMDF along $\mathbf{r}(t)$ depends only on $\mathbf{o}(t)$, not on the polar

distance $|\mathbf{r}(t)|$ from the origin. Hence, for a given polar indicatrix $\mathbf{o}(t)$ and any polynomial $\rho(t)$ that is positive on $[\,0,\,1\,]$, the curves defined by

$$\boldsymbol{\rho}(t) \;=\; \rho(t)\,\mathbf{o}(t) \tag{4}$$

have identical RMDFs. The polynomial $\rho(t)$ can be used to specify the polar distance of $\boldsymbol{\rho}(t)$ from the origin, without altering its RMDF. In view of this, we employ the following procedure to construct the desired interpolant $\boldsymbol{\rho}(t)$.

1. Compute a P curve $\mathbf{r}(t)$ of degree ≤ 4 (see Section 4) with a rational RMDF satisfying $\mathbf{r}(t) \neq \mathbf{0}$ for $t \in [\,0,\,1\,]$ such that

$$\mathbf{r}(0) \;=\; \mathbf{o}_i\,, \qquad \mathbf{r}(1) \;=\; \lambda\,\mathbf{o}_f\,, \tag{5}$$

$$\begin{cases} (\mathbf{o}(0),\,\mathbf{u}(0),\,\mathbf{v}(0)) \;=\; (\mathbf{o}_i,\,\mathbf{u}_i,\,\mathbf{v}_i)\,, \\ (\mathbf{o}(1),\,\mathbf{u}(1),\,\mathbf{v}(1)) \;=\; (\mathbf{o}_f,\,\mathbf{u}_f,\,\mathbf{v}_f)\,, \end{cases} \tag{6}$$

$$\mathbf{r}'(0) \;=\; \mu\,\mathbf{f}_i\,, \tag{7}$$

   where λ and μ are positive free parameters, and $(\mathbf{o}(t), \mathbf{u}(t), \mathbf{v}(t))$ is the rational RMDF associated with $\mathbf{r}(t)$;
2. define the associated rational polar indicatrix $\mathbf{o}(t) = \mathbf{r}(t)/|\mathbf{r}(t)|$ on the unit sphere—see Section 5;
3. define the interpolant to conditions (1)–(2) by (4) with rational RMDF $(\mathbf{o}(t), \mathbf{u}(t), \mathbf{v}(t))$ by computing a suitable polynomial $\rho(t)$, positive for $t \in [\,0,\,1\,]$—see Section 6.

3 Polynomial curves with rational RMDF

The distinctive property of a polynomial Pythagorean (P) curve $\mathbf{r}(t)$ is that its polar distance $|\mathbf{r}(t)|$ is a *polynomial* in the curve parameter t. Since this is equivalent to the requirement that its anti-hodograph is a PH curve, a P curve can be generated [7] by a quaternion product of the form

$$\mathbf{r}(t) \;=\; \mathcal{A}(t)\,\mathbf{i}\,\mathcal{A}^*(t)\,, \tag{8}$$

where $\mathcal{A}(t) = u(t) + v(t)\,\mathbf{i} + p(t)\,\mathbf{j} + q(t)\,\mathbf{k}$ is a quaternion polynomial of degree m for a P curve of degree $n = 2m$, and $\mathcal{A}^*(t) = u(t) - v(t)\,\mathbf{i} - p(t)\,\mathbf{j} - q(t)\,\mathbf{k}$ is its conjugate.[2] To obtain sufficient degrees of freedom, we focus on the case $\deg(\mathcal{A}(t)) = 2$—i.e., quartic P curves defined by substituting a quadratic quaternion polynomial

$$\mathcal{A}(t) \;=\; \mathcal{A}_0\,(1-t)^2 \;+\; \mathcal{A}_1\,2\,(1-t)\,t \;+\; \mathcal{A}_2\,t^2 \tag{9}$$

[2]The scalar and vector parts of a quaternion $\mathcal{A} = (a, \mathbf{a})$ are denoted by $a = \mathrm{scal}(\mathcal{A})$ and $\mathbf{a} = \mathrm{vect}(\mathcal{A})$—see Chapter 5 of [5] for an appropriate review of the quaternion algebra.

into (8). The control points $\mathbf{p}_i = x_i\,\mathbf{i} + y_i\,\mathbf{j} + z_i\,\mathbf{k}$ of the Bézier form

$$\mathbf{r}(t) \;=\; \sum_{i=0}^{4} \mathbf{p}_i \binom{4}{i} (1-t)^{4-i}\, t^i \tag{10}$$

are then given by

$$\begin{aligned}
\mathbf{p}_0 &= \mathcal{A}_0\,\mathbf{i}\,\mathcal{A}_0^*\,,\\
\mathbf{p}_1 &= \frac{1}{2}\left(\mathcal{A}_0\,\mathbf{i}\,\mathcal{A}_1^* + \mathcal{A}_1\,\mathbf{i}\,\mathcal{A}_0^*\right),\\
\mathbf{p}_2 &= \frac{1}{6}\left(\mathcal{A}_0\,\mathbf{i}\,\mathcal{A}_2^* + 4\,\mathcal{A}_1\,\mathbf{i}\,\mathcal{A}_1^* + \mathcal{A}_2\,\mathbf{i}\,\mathcal{A}_0^*\right),\\
\mathbf{p}_3 &= \frac{1}{2}\left(\mathcal{A}_1\,\mathbf{i}\,\mathcal{A}_2^* + \mathcal{A}_2\,\mathbf{i}\,\mathcal{A}_1^*\right),\\
\mathbf{p}_4 &= \mathcal{A}_2\,\mathbf{i}\,\mathcal{A}_2^*\,.
\end{aligned} \tag{11}$$

Remark 1 Rational curves on the unit sphere (or rational *spherical curves*) play an important role in geometric design, animation, motion planning, and related problems. By interpreting such a curve as a tangent indicatrix and augmenting it with a rational support function, for example, one can define *rational PH space curves* [12]. The P curves specified by (8) may be regarded as the numerators of such rational spherical curves.

Now the set of P quartics that have rational RMDFs can be identified by analogy with the set of PH quintics that have rational RMAFs [7]. Namely, the curve (10) has a rational RMDF if and only if the quaternion coefficients of (9) satisfy [6] the vector constraint

$$\mathcal{A}_1\,\mathbf{i}\,\mathcal{A}_1^* \;=\; \mathrm{vect}\big(\mathcal{A}_2\,\mathbf{i}\,\mathcal{A}_0^*\big)\,. \tag{12}$$

By analogy with the analysis of rational RMAFs on PH quintics in [10], the rational RMDF on a P quartic satisfying this constraint can be defined as

$$(\mathbf{o}(t), \mathbf{u}(t), \mathbf{v}(t)) \;=\; \frac{(\mathcal{B}(t)\,\mathbf{i}\,\mathcal{B}^*(t),\, \mathcal{B}(t)\,\mathbf{j}\,\mathcal{B}^*(t),\, \mathcal{B}(t)\,\mathbf{k}\,\mathcal{B}^*(t))}{|\mathcal{B}(t)|^2}\,, \tag{13}$$

where $\mathcal{B}(t) = \mathcal{A}(t)\mathcal{W}^*(t)$, and the coefficients of

$$\mathcal{W}(t) \;=\; \mathcal{W}_0(1-t)^2 + \mathcal{W}_1\,2(1-t)t + \mathcal{W}_2 t^2 \tag{14}$$

must be expressed in terms of $\mathcal{A}_0$, $\mathcal{A}_1$, $\mathcal{A}_2$ to capture the RMDF. One may, without loss of generality, set $\mathcal{W}_0 = 1$, and the initial RMDF at $t = 0$ is then coincident with the *Euler–Rodrigues frame* [2]. The remaining coefficients $\mathcal{W}_1$, $\mathcal{W}_2$ have known expressions in terms of the Hopf map form of PH curves [9], which can be translated to the quaternion form as

$$\mathcal{W}_1 \;=\; \frac{\left(\mathcal{A}_0^*\,\mathcal{A}_1\right)_{1,\mathbf{i}}}{|\mathcal{A}_0|^2} \qquad \text{and} \qquad \mathcal{W}_2 \;=\; \frac{\left(\mathcal{A}_0^*\,\mathcal{A}_1\right)_{1,\mathbf{i}} \left(\mathcal{A}_1^*\,\mathcal{A}_2\right)_{1,\mathbf{i}}}{|\left(\mathcal{A}_0^*\,\mathcal{A}_1\right)_{1,\mathbf{i}}|^2}\,,$$

where

$$(\mathcal{A})_{1,\mathbf{i}} \;=\; \frac{1}{2}(\mathcal{A} - \mathbf{i}\,\mathcal{A}\,\mathbf{i})$$

denotes the quaternion obtained from $\mathcal{A}$ by deleting its $\mathbf{j}$, $\mathbf{k}$ components—i.e., $(\mathcal{A})_{1,\mathbf{i}} = u + v\,\mathbf{i}$ if $\mathcal{A} = u + v\,\mathbf{i} + p\,\mathbf{j} + q\,\mathbf{k}$ (note that the coefficients of (14) are just complex numbers if we identify $\mathbf{i}$ with the imaginary unit i).

4 Quartic P curve with rational RMDF

We begin by constructing a quartic P curve $\mathbf{r}(t)$ that interpolates the given data (5)–(7) and satisfies the condition (12) for existence of a rational RMDF. The rational polar indicatrix $\mathbf{o}(t) = \mathbf{r}(t)/|\mathbf{r}(t)|$ corresponding to $\mathbf{r}(t)$ then has the same rational RMDF as $\mathbf{r}(t)$—see Section 5.

Without loss of generality, we take $(\mathbf{o}_i, \mathbf{u}_i, \mathbf{v}_i) = (\mathbf{i}, -\mathbf{j}, -\mathbf{k})$ as the initial frame, and for brevity we set

$$\mathbf{g}_i \;=\; \mathbf{i}\times\mathbf{f}_i\,. \tag{15}$$

Note that $(\mathbf{i}, \mathbf{f}_i, \mathbf{g}_i)$ define a right-handed orthonormal basis. Conditions (5) and (7) then yield the quaternion equations

$$\mathcal{A}_0\,\mathbf{i}\,\mathcal{A}_0^* \;=\; \mathbf{i}\,, \qquad \mathcal{A}_2\,\mathbf{i}\,\mathcal{A}_2^* \;=\; \lambda\,\mathbf{o}_f\,, \tag{16}$$

and $2(\mathcal{A}_1 - \mathcal{A}_0)\,\mathbf{i}\,\mathcal{A}_0^* + \mathcal{A}_0\,\mathbf{i}\,2(\mathcal{A}_1^* - \mathcal{A}_0^*) = \mu\,\mathbf{f}_i$, which reduces to

$$2\big(\mathcal{A}_0\,\mathbf{i}\,\mathcal{A}_1^* + \mathcal{A}_1\,\mathbf{i}\,\mathcal{A}_0^*\big) \;=\; \mu\,\mathbf{f}_i + 4\,\mathbf{i}\,. \tag{17}$$

The solutions of equations (16) can be expressed [8] in terms of free angular parameters ϕ_0 and ϕ_2 as

$$\mathcal{A}_0 \;=\; \mathbf{i}\,(\cos\phi_0 + \mathbf{i}\sin\phi_0)\,, \qquad \mathcal{A}_2 \;=\; \sqrt{\lambda}\,\mathbf{n}_2\,(\cos\phi_2 + \mathbf{i}\sin\phi_2)\,, \tag{18}$$

where $\mathbf{n}_2$ is the unit bisector of $\mathbf{i}$ and $\mathbf{o}_f$, defined by

$$\mathbf{n}_2 \;=\; \frac{\mathbf{o}_f + \mathbf{i}}{|\,\mathbf{o}_f + \mathbf{i}\,|} \quad \text{if } \mathbf{o}_f \neq -\mathbf{i}\,, \qquad \mathbf{n}_2 \;=\; \mathbf{j} \quad \text{if } \mathbf{o}_f = -\mathbf{i}\,. \tag{19}$$

Note that $\mathbf{n}_2\times\mathbf{i} \neq \mathbf{0}$ if $\mathbf{o}_f \neq \mathbf{i}$. For later use, we also observe that the unit bisector of $\mathbf{i}$ and $\mathbf{o}_i = \mathbf{i}$ is just $\mathbf{n}_0 = \mathbf{i}$.

Invoking the analogy between rational RMDFs on P curves and rational RMAFs on PH curves, the angles ϕ_0, ϕ_2 can be determined as described in [10] to satisfy interpolation of the given end-frames $(\mathbf{o}_i, \mathbf{u}_i, \mathbf{v}_i)$ and $(\mathbf{o}_f, \mathbf{u}_f, \mathbf{v}_f)$. As noted in [10], this problem admits solutions for arbitrary end-frames when $\mathbf{o}_f \neq \mathbf{i}$. In particular, there are four pairs of admissible (ϕ_0, ϕ_2) values which—for the choice $(\mathbf{o}_i, \mathbf{u}_i, \mathbf{v}_i) = (\mathbf{i}, -\mathbf{j}, -\mathbf{k})$—are of the form

$$(0, \beta_A)\,, \qquad (\pi, \pi + \beta_A)\,, \qquad (0, \beta_B)\,, \qquad (\pi, \pi + \beta_B)\,.$$

The two possible differences $\phi_2 - \phi_0 = \beta_A$ and $\phi_2 - \phi_0 = \beta_B$ (corresponding to the first and last two cases above) are analyzed below, writing β to denote

β_A or β_B (see the Appendix for details of their computation). Furthermore, the analysis below shows that one can take $\phi_0 = 0$ without loss of generality, so there are only two alternatives for the P quartic interpolant.

First, we note that $\mathcal{A}_0 = \pm\mathbf{i}$ if $\phi_0 = 0$ or $\phi_0 = \pi$, and hence

$$\begin{aligned} \mathcal{A}_0\,\mathbf{i}\,\mathcal{A}_1^* + \mathcal{A}_1\,\mathbf{i}\,\mathcal{A}_0^* &= \pm\big(\mathcal{A}_1 - \mathcal{A}_1^*\big) = \pm 2\,\mathrm{vect}(\mathcal{A}_1)\,, \\ \mathcal{A}_0\,\mathbf{i}\,\mathcal{A}_2^* + \mathcal{A}_2\,\mathbf{i}\,\mathcal{A}_0^* &= \pm\big(\mathcal{A}_2 - \mathcal{A}_2^*\big) = \pm 2\,\mathrm{vect}(\mathcal{A}_2)\,. \end{aligned} \tag{20}$$

We now impose the rational RMDF condition (12). Substituting the second relation above into (12) and using (18), we obtain

$$\mathcal{A}_1\,\mathbf{i}\,\mathcal{A}_1^* = \pm\,\mathrm{vect}(\mathcal{A}_2) = \sqrt{\lambda}\,\mathbf{w}\,, \tag{21}$$

with

$$\mathbf{w} = \cos\beta\,\mathbf{n}_2 + \sin\beta\,\mathbf{n}_2\times\mathbf{i}\,, \tag{22}$$

where we use the fact that $\phi_2 = \beta$ if $\phi_0 = 0$ and $\phi_2 = \beta + \pi$ if $\phi_0 = \pi$. The solution of (21) may be expressed in terms of a free angular parameter ϕ_1 as

$$\mathcal{A}_1 = \sqrt[4]{\lambda}\,\sqrt{|\mathbf{w}|}\,\mathbf{n}_1\,(\cos\phi_1 + \mathbf{i}\sin\phi_1)\,, \tag{23}$$

where

$$\mathbf{n}_1 = \frac{\mathbf{w} + |\mathbf{w}|\,\mathbf{i}}{|\,\mathbf{w} + |\mathbf{w}|\,\mathbf{i}\,|} \tag{24}$$

is the unit bisector of $\mathbf{i}$ and $\mathbf{w}/|\mathbf{w}|$. Consequently, we have

$$\mathrm{vect}(\mathcal{A}_1) = \sqrt[4]{\lambda}\,(\cos\phi_1\mathbf{w}_1 + \sin\phi_1\mathbf{w}_2)\,, \tag{25}$$

where

$$\mathbf{w}_1 = \sqrt{|\mathbf{w}|}\,\mathbf{n}_1\,, \qquad \mathbf{w}_2 = \sqrt{|\mathbf{w}|}\,\mathbf{n}_1\times\mathbf{i}\,. \tag{26}$$

The following lemma shows that when $\mathbf{o}_f \neq \mathbf{i}$, we have $\mathbf{w} \neq \mathbf{0}$ and $\mathbf{w}\times\mathbf{i} \neq \mathbf{0}$, so $\mathbf{n}_1$ and $\mathcal{A}_1$ are well-defined, and certain degenerate cases are avoided.

Lemma 1 *When $\mathbf{o}_f \neq \mathbf{i}$, the vectors $\mathbf{w}$, $\mathbf{w}\times\mathbf{i}$, $\mathbf{w}_1$, $\mathbf{w}_2$, and $\mathbf{g}_i\times(\mathbf{w}_1\times\mathbf{w}_2)$ are all non-vanishing.*

Proof From (19) we observe that $\mathbf{n}_2$ and $\mathbf{n}_2\times\mathbf{i}$ are non-zero and linearly independent when $\mathbf{o}_f \neq \mathbf{i}$, and expression (22) then implies that $\mathbf{w} \neq \mathbf{0}$ for all β. Now if $\mathbf{w}\times\mathbf{i} = \mathbf{0}$ with $\mathbf{w} \neq \mathbf{0}$, we must have $\mathbf{w} = \zeta\,\mathbf{i}$ with $\zeta \neq 0$. Setting $\mathbf{w} = \zeta\,\mathbf{i}$ in (22) and taking dot products with $\mathbf{i}$ and $\mathbf{n}_2$ gives $\cos\beta\,(\mathbf{i}\cdot\mathbf{n}_2) = \zeta$ and $\cos\beta = \zeta\,(\mathbf{i}\cdot\mathbf{n}_2)$, which together imply that $(\mathbf{i}\cdot\mathbf{n}_2)^2 = 1$. From (19) this is possible only if $\mathbf{n}_2 = \mathbf{i}$, i.e., $\mathbf{o}_f = \mathbf{i}$. Hence, $\mathbf{w}\times\mathbf{i} \neq \mathbf{0}$ when $\mathbf{o}_f \neq \mathbf{i}$.

Now $\mathbf{w}_1 = \mathbf{0}$ implies that $\mathbf{n}_1 = \mathbf{0}$—i.e., $\mathbf{w} = -\,|\mathbf{w}|\,\mathbf{i}$, since $|\mathbf{w}| \neq 0$. This amounts to the case $\zeta = -\,|\mathbf{w}|$ of the preceding argument, and is impossible when $\mathbf{o}_f \neq \mathbf{i}$. Similarly, $\mathbf{w}_2 = \mathbf{0}$ implies that $\mathbf{n}_1\times\mathbf{i} = \mathbf{0}$, and thus $\mathbf{w}\times\mathbf{i} = \mathbf{0}$, which has been ruled out when $\mathbf{o}_f \neq \mathbf{i}$. Finally, $\mathbf{g}_i\times(\mathbf{w}_1\times\mathbf{w}_2) = \mathbf{0}$ implies that $\mathbf{g}_i\times(\mathbf{n}_1\times(\mathbf{n}_1\times\mathbf{i})) = \mathbf{g}_i\times[\,(\mathbf{i}\cdot\mathbf{n}_1)\mathbf{n}_1 - \mathbf{i}\,] = \mathbf{0}$. Since $\mathbf{g}_i$ is orthogonal to $\mathbf{i}$, this is

equivalent to $\mathbf{i} \cdot [\, (\mathbf{i} \cdot \mathbf{n}_1)\mathbf{n}_1 - \mathbf{i}\,] = 0$, i.e., $(\mathbf{i} \cdot \mathbf{n}_1)^2 = 1$. From (24), this corresponds to $\mathbf{w} = |\mathbf{w}|\,\mathbf{i}$, contradicting $\mathbf{w} \times \mathbf{i} \neq \mathbf{0}$ when $\mathbf{o}_f \neq \mathbf{i}$. □

Having solved (16), we turn to condition (17). Invoking the first relation in (20), this becomes

$$\pm\,\mathrm{vect}(\mathcal{A}_1) \;=\; \frac{\mu}{4}\,\mathbf{f}_i + \mathbf{i}\,. \tag{27}$$

From (15) we see that, since μ is a positive parameter, this is equivalent to

$$\mathrm{vect}(\mathcal{A}_1) \cdot \mathbf{g}_i \;=\; 0\,, \qquad \pm\,\mathrm{vect}(\mathcal{A}_1) \cdot \mathbf{i} \;=\; 1\,, \tag{28}$$

and

$$\frac{\mu}{4} \;=\; \pm\,\mathrm{vect}(\mathcal{A}_1) \cdot \mathbf{f}_i \;>\; 0\,. \tag{29}$$

Using (25), conditions (28) can be written as a pair of linear equations

$$\begin{bmatrix} \mathbf{w}_1 \cdot \mathbf{g}_i & \mathbf{w}_2 \cdot \mathbf{g}_i \\ \mathbf{w}_1 \cdot \mathbf{i} & \mathbf{w}_2 \cdot \mathbf{i} \end{bmatrix} \begin{bmatrix} \cos\phi_1 \\ \sin\phi_1 \end{bmatrix} = \begin{bmatrix} 0 \\ \pm 1/\sqrt[4]{\lambda} \end{bmatrix} \tag{30}$$

in $\cos\phi_1$, $\sin\phi_1$. Now from (26) we have $\mathbf{w}_2 \cdot \mathbf{i} = 0$. Also, from (24) and (26) we obtain $\mathbf{w}_1 \cdot \mathbf{i} > 0$ (since $\mathbf{w}_1 \cdot \mathbf{i} = 0$ implies that $\mathbf{w} = -\,|\mathbf{w}|\,\mathbf{i}$ which in turn implies $\mathbf{w} \times \mathbf{i} = \mathbf{0}$, and this was ruled out in Lemma 1).

Now Lemma 1 implies that the first of equations (30) is non-trivial, since $\mathbf{w}_1 \cdot \mathbf{g}_i = \mathbf{w}_2 \cdot \mathbf{g}_i = 0 \;\Rightarrow\; \mathbf{g}_i = \zeta\, \mathbf{w}_1 \times \mathbf{w}_2$ for some ζ, contradicting the fact that $\mathbf{g}_i \times (\mathbf{w}_1 \times \mathbf{w}_2) \neq \mathbf{0}$. Thus, a solution of the system (30) exists if and only if $\mathbf{w}_2 \cdot \mathbf{g}_i \neq 0$. Concerning this, we note from (26) that $\mathbf{w}_2 \cdot \mathbf{g}_i = 0$ if and only if $\mathbf{n}_1 \cdot \mathbf{f}_i = 0$, and from (24) this is possible if and only if $\mathbf{w} \cdot \mathbf{f}_i = 0$. Hence, the condition for the existence of a solution to (30) can be written as

$$\mathbf{w} \cdot \mathbf{f}_i \;\neq\; 0\,.$$

Recalling that $(\mathbf{i}, \mathbf{f}_i, \mathbf{g}_i)$ define a right-handed orthonormal basis, and using (19) and (22), this can be re-written when $\mathbf{o}_f \neq -\,\mathbf{i}$ as[3]

$$\mathbf{o}_f \cdot \mathbf{f}_i\, \cos\beta \;+\; \mathbf{o}_f \cdot \mathbf{g}_i\, \sin\beta \;\neq\; 0\,, \tag{31}$$

which always admits a solution β under the assumption that $\mathbf{o}_f \neq \pm\mathbf{i}$, since $\mathbf{o}_f \cdot \mathbf{g}_i = \mathbf{o}_f \cdot \mathbf{f}_i = 0$ is impossible because $(\mathbf{i}, \mathbf{f}_i, \mathbf{g}_i)$ are orthonormal vectors.

When (31) is satisfied, the unique solution to (30) can be written as

$$\cos\phi_1 \;=\; \pm\,\frac{1}{\sqrt[4]{\lambda}}\,\frac{1}{\mathbf{w}_1 \cdot \mathbf{i}}\,, \qquad \sin\phi_1 \;=\; \mp\,\frac{1}{\sqrt[4]{\lambda}}\,\frac{\mathbf{w}_1 \cdot \mathbf{g}_i}{(\mathbf{w}_2 \cdot \mathbf{g}_i)(\mathbf{w}_1 \cdot \mathbf{i})}\,. \tag{32}$$

The value of the positive parameter λ is then determined by requiring that $\cos^2\phi_1 + \sin^2\phi_1 = 1$, which gives

$$\lambda \;=\; \left[\, \frac{(\mathbf{w}_1 \cdot \mathbf{g}_i)^2 + (\mathbf{w}_2 \cdot \mathbf{g}_i)^2}{(\mathbf{w}_1 \cdot \mathbf{i})^2 (\mathbf{w}_2 \cdot \mathbf{g}_i)^2} \,\right]^2\,. \tag{33}$$

[3] In the special case $\mathbf{o}_f = -\,\mathbf{i}$, it becomes $\mathbf{j} \cdot \mathbf{f}_i\, \cos\beta + \mathbf{j} \cdot \mathbf{g}_i\, \sin\beta \neq 0$.

Now since the solutions (32) differ only in sign, if ϕ_1 is the angle associated with $(\phi_0, \phi_2) = (0, \beta)$, the angle associated with $(\phi_0, \phi_2) = (\pi, \pi + \beta)$ is just $\pi + \phi_1$. Also, since the values $(\phi_0, \phi_1, \phi_2) = (\pi, \pi + \phi_1, \pi + \beta)$ generate exactly the same curve as $(0, \phi_1, \beta)$ we may set $\phi_0 = 0$ without loss of generality.

Finally, condition (29) becomes $\pm \sqrt[4]{\lambda}\,(\mathbf{w}_1 \cdot \mathbf{f}_i \cos\phi_1 + \mathbf{w}_2 \cdot \mathbf{f}_i \sin\phi_1) > 0$, and using (32) this is equivalent to

$$\frac{\mu}{4} = \frac{(\mathbf{w}_1 \cdot \mathbf{f}_i)(\mathbf{w}_2 \cdot \mathbf{g}_i) - (\mathbf{w}_2 \cdot \mathbf{f}_i)(\mathbf{w}_1 \cdot \mathbf{g}_i)}{(\mathbf{w}_1 \cdot \mathbf{i})(\mathbf{w}_2 \cdot \mathbf{g}_i)} > 0\,,$$

or (since $\mathbf{i}, \mathbf{f}_i, \mathbf{g}_i$ are mutually orthogonal unit vectors)

$$\frac{\mu}{4} = \frac{(\mathbf{w}_1 \times \mathbf{w}_2) \cdot \mathbf{i}}{(\mathbf{w}_1 \cdot \mathbf{i})\,(\mathbf{w}_2 \cdot \mathbf{g}_i)} > 0\,. \tag{34}$$

From (26) one can verify that the numerator of the above expression has the negative value $-|\mathbf{w}|\,|\mathbf{n}_1 \times \mathbf{i}|^2$ (which can not vanish). Hence, since $\mathbf{w}_1 \cdot \mathbf{i} > 0$, this inequality becomes simply $\mathbf{w}_2 \cdot \mathbf{g}_i < 0$, and from (15), (24), and (26) one can deduce that this is equivalent to

$$\mathbf{w} \cdot \mathbf{f}_i > 0\,,$$

which, when $\mathbf{o}_f \neq -\mathbf{i}$, can be re-written as[4]

$$\mathbf{o}_f \cdot \mathbf{f}_i \cos\beta + \mathbf{o}_f \cdot \mathbf{g}_i \sin\beta > 0\,, \tag{35}$$

which evidently reinforces (31). This can be regarded as a restriction on the final frame orientation $(\mathbf{o}_f, \mathbf{u}_f, \mathbf{v}_f)$, relative to the initial frame $(\mathbf{o}_i, \mathbf{u}_i, \mathbf{v}_i) = (\mathbf{i}, -\mathbf{j}, -\mathbf{k})$. In terms of the angle $\beta_* \in [0\,,\ 2\pi)$ uniquely defined by

$$(\sin\beta_*, \cos\beta_*) = \frac{(\mathbf{o}_f \cdot \mathbf{f}_i, \mathbf{o}_f \cdot \mathbf{g}_i)}{\sqrt{(\mathbf{o}_f \cdot \mathbf{f}_i)^2 + (\mathbf{o}_f \cdot \mathbf{g}_i)^2}}\,, \tag{36}$$

the inequality (35) can be written as $\sqrt{(\mathbf{o}_f \cdot \mathbf{f}_i)^2 + (\mathbf{o}_f \cdot \mathbf{g}_i)^2}\,\sin(\beta_* + \beta) > 0$, and hence it is satisfied when

$$\beta \in (-\beta_*, \pi - \beta_*)\,. \tag{37}$$

We now give sufficient conditions on the end frame orientations ensuring that (35) holds for exactly one of the values β_A or β_B. To state these conditions, we introduce [10] the vectors $\mathbf{j}_0, \mathbf{j}_2$ and $\mathbf{k}_0, \mathbf{k}_2$ defined by

$$\mathbf{j}_r = 2(\mathbf{j} \cdot \mathbf{n}_r)\mathbf{n}_r - \mathbf{j}\,, \qquad \mathbf{k}_r = 2(\mathbf{k} \cdot \mathbf{n}_r)\mathbf{n}_r - \mathbf{k} \tag{38}$$

for $r = 0, 2$. These are simply the reflections of $\mathbf{j}$ and $\mathbf{k}$ in $\mathbf{n}_0, \mathbf{n}_2$. We also define [10] the parameter

$$\delta = \mathbf{n}_0 \cdot \mathbf{n}_2\,, \tag{39}$$

and we set

$$\hat{\eta} = \arg(\delta + \mathrm{i}\sqrt{1 - \delta^2})\,. \tag{40}$$

[4] In the special case $\mathbf{o}_f = -\mathbf{i}$, it becomes $\mathbf{j} \cdot \mathbf{f}_i \cos\beta + \mathbf{j} \cdot \mathbf{g}_i \sin\beta > 0$.

Since it is rather technical, the proof of the following result is deferred to the Appendix (which also treats the special cases $\mathbf{o}_f \cdot \mathbf{f}_i = 0$ and $\mathbf{o}_f \cdot \mathbf{g}_i = 0$).

Proposition 1 *Suppose that* $\mathbf{o}_f \cdot \mathbf{f}_i \neq 0$ *and* $\mathbf{o}_f \cdot \mathbf{g}_i \neq 0$, *and let* $\hat{\eta}$ *be defined by* (40). *Then if the inequalities*

$$(\mathbf{o}_f \cdot \mathbf{f}_i)(\mathbf{o}_f \cdot \mathbf{g}_i)(\mathbf{j}_2 \cdot \mathbf{v}_f) \;\leq\; 0\,, \qquad \mathbf{k}_2 \cdot \mathbf{v}_f \;\geq\; \cos 2\hat{\eta} \tag{41}$$

hold, exactly one of the two values β_A, β_B *satisfies* (35).

Conditions (41) on the final frame orientation in Proposition 1 correspond geometrically to requiring that the frame vector $\mathbf{v}_f$ should lie in one of two half-spaces, defined by the intersection of the volumes bounded by the plane orthogonal to $\mathbf{j}_2$, and the cone with axis $\mathbf{k}_2$ and half-angle $2\hat{\eta}$. Note also that the conditions of Proposition 1 become more stringent when $\delta \approx 1$, i.e., when $\mathbf{o}_f$ approaches $\mathbf{o}_i = \mathbf{i}$, since then $\hat{\eta} \approx 0$. Finally, a significant case in which the assumptions of this proposition hold is when $\mathbf{o}_f \cdot \mathbf{f}_i \neq 0$ and $\mathbf{u}_f = \mathbf{j}_2$, $\mathbf{v}_f = \mathbf{k}_2$ since we then have[5] $\mathbf{k}_2 \cdot \mathbf{v}_f = 1$ and $\mathbf{j}_2 \cdot \mathbf{v}_f = 0$.

Finally, to ensure a well-defined polar indicatrix $\mathbf{o}(t) = \mathbf{r}(t)/|\mathbf{r}(t)|$ on the unit sphere from $\mathbf{r}(t)$, we verify that $|\mathbf{r}(t)| \neq 0$ for $t \in [\,0, 1\,]$ as follows.

Proposition 2 $\mathbf{r}(t) \neq \mathbf{0}$ *for* $t \in [\,0, 1\,]$ *when* $\mathbf{i} \neq \mathbf{o}_f$.

Proof Since $\mathbf{r}(0) = \mathbf{i}$ and $\mathbf{r}(1) = \lambda\,\mathbf{o}_f$ with $\lambda > 0$, we need only consider $t \in (0, 1)$. Now $|\mathbf{r}(t)| = |\mathcal{A}(t)|^2$, so $\mathbf{r}(t) \neq \mathbf{0}$ for $t \in (0, 1)$ if and only if $\mathcal{A}(t)$ is non-vanishing on $(0, 1)$. For (9) to vanish at some point $t \in (0, 1)$ a positive value $\tau = (1 - t)/t$ must exist, such that

$$2\mathcal{A}_1 \;=\; \tau\,\mathcal{A}_0 \,+\, \frac{\mathcal{A}_2}{\tau}\,.$$

Substituting into the rational RMDF constraint (12) and using $\mathcal{A}_0\,\mathbf{i}\,\mathcal{A}_0^* = \mathbf{i}$, $\mathcal{A}_2\,\mathbf{i}\,\mathcal{A}_2^* = \lambda\,\mathbf{o}_f$, and (21) then gives

$$\mathbf{w} \;=\; \frac{1}{2}\left(\frac{\tau^2}{\sqrt{\lambda}}\,\mathbf{i} \,+\, \frac{\sqrt{\lambda}}{\tau^2}\,\mathbf{o}_f\right). \tag{42}$$

Now from (19) $\mathbf{n}_2 \times \mathbf{i} \neq \mathbf{0}$ when $\mathbf{o}_f \neq \mathbf{i}$, and (22) then implies that $\mathbf{w}$ depends linearly on $\mathbf{i}$ and $\mathbf{o}_f$ only when $\beta = 0$ or π. Thus (42) cannot be satisfied in the general case. In the special cases $\beta = 0$ or π, we have $\mathbf{w} = \pm\mathbf{n}_2$ from (22), and it is also necessary that $\tau^2/\sqrt{\lambda} = \sqrt{\lambda}/\tau^2$—i.e., $\lambda = \tau^4$—for (42) to be satisfied. However, this implies that $\mathbf{w} = \frac{1}{2}\,(\mathbf{i} + \mathbf{o}_f)$, which is incompatible with the case

[5] In this case, since $\mathbf{u}_i = \mathbf{j}_0 = -\,\mathbf{j}$ and $\mathbf{v}_i = \mathbf{k}_0 = -\,\mathbf{k}$, the initial and final frames are obtained by reflecting $\mathbf{i}, \mathbf{j}, \mathbf{k}$ in $\mathbf{n}_0 = \mathbf{i}$ and $\mathbf{n}_2$, respectively.

$\beta = \pi$. In the case $\beta = 0$, we must have $|\mathbf{i} + \mathbf{o}_f| = 2$, and this is impossible if $\mathbf{i} \neq \mathbf{o}_f$. □

5 Interpolation on the unit sphere

Based on the analysis of the previous section, the polar indicatrix of $\mathbf{r}(t)$ on the unit sphere can be defined as $\mathbf{o}(t) = \mathbf{r}(t)/|\mathbf{r}(t)|$. As noted in Section 2, the previously defined RMDF $(\mathbf{o}(t), \mathbf{u}(t), \mathbf{v}(t))$ for $\mathbf{r}(t)$ is also an RMF for $\mathbf{o}(t)$, and it is such that conditions (6) hold. In addition, since

$$\mathbf{o}'(t) \;=\; \frac{\mathbf{r}'(t) - (\mathbf{o}(t) \cdot \mathbf{r}'(t))\,\mathbf{o}(t)}{|\mathbf{r}(t)|}\,,$$

we see that

$$\mathbf{o}'(0) \;=\; \mathbf{r}'(0) \;=\; \mu\,\mathbf{f}_i\,, \tag{43}$$

μ being the positive constant defined in (34), and $\mathbf{f}_i$ the unit vector orthogonal to $\mathbf{o}_i$ defined by (3). The following summarizes the procedure for computing at most 2 curves $\mathbf{o}(t)$ on the unit sphere, satisfying the prescribed interpolation conditions.

input: $(\mathbf{o}_i, \mathbf{u}_i, \mathbf{v}_i) = (\mathbf{i}, -\mathbf{j}, -\mathbf{k})$, $(\mathbf{o}_f, \mathbf{u}_f, \mathbf{v}_f)$, $\mathbf{f}_i$

1. set $\mathbf{g}_i = \mathbf{i} \times \mathbf{f}_i$ and define $\mathbf{n}_2$ through (19);
2. *end-frame interpolation*: determine the two admissible values β_A, β_B for $\beta = \phi_2 - \phi_0$ as outlined in the Appendix—see also [10];
3. for each β value, set $\phi_0 = 0$ and $\phi_2 = \beta$ and proceed as follows:
   (a) define the vectors $\mathbf{w}$ and $\mathbf{n}_1$ by expressions (22) and (24);
   (b) define the vectors $\mathbf{w}_1$ and $\mathbf{w}_2$ through expressions (26);
   (c) if the inequality (35) is not satisfied, return to step 3 and choose the other β value;
   (d) determine the quaternion coefficients $\mathcal{A}_0$, $\mathcal{A}_2$ from (18);
   (e) determine the parameter λ from (33);
   (f) determine the angle ϕ_1 from (32);
   (g) compute the quaternion coefficient $\mathcal{A}_1$ from (23);
   (h) compute the Bézier control points $\mathbf{p}_0, \ldots, \mathbf{p}_4$ from (11);
   (i) determine the quartic P curve $\mathbf{r}(t)$ from (10) and its associated rational RMDF $(\mathbf{o}(t), \mathbf{u}(t), \mathbf{v}(t))$ from (13);
   (j) define the polar indicatrix $\mathbf{o}(t) = \mathbf{r}(t)/|\mathbf{r}(t)|$.

output: at most 2 curves $\mathbf{o}(t)$ on the unit sphere with associated rational RMDFs $(\mathbf{o}(t), \mathbf{u}(t), \mathbf{v}(t))$ that satisfy (6) and (43).

When two curves $\mathbf{o}(t)$ exist, a suitable shape measure may be invoked to select a preferred solution among them—for example, one might prefer the

solution with the least (maximum or root-mean-square) deviation from the great-circle arc connecting the end-points $\mathbf{o}_i$ and $\mathbf{o}_f$.

6 End-point/tangent interpolation

As noted in Section 2, any curve defined as $\boldsymbol{\rho}(t) = \rho(t)\,\mathbf{o}(t)$ with $\rho(t) \neq 0$ has the same RMDF as $\mathbf{o}(t)$. If the curve $\mathbf{o}(t)$ on the unit sphere is computed as described above, $\boldsymbol{\rho}(t)$ will interpolate the prescribed initial/final frames.

In general $\boldsymbol{\rho}(t)$ will be a rational curve whenever $\rho(t)$ is a rational function. For simplicity, we consider here the case where $\rho(t)$ is a polynomial of degree $k \geq 2$, expressed in Bernstein form as

$$\rho(t) \;=\; \sum_{i=0}^{k} \rho_i \binom{k}{i} (1-t)^{k-i} t^i \,. \tag{44}$$

The end-point conditions $\boldsymbol{\rho}(0) = d_i\,\mathbf{o}_i$, $\boldsymbol{\rho}(1) = d_f\,\mathbf{o}_f$ are then satisfied with

$$\rho_0 \;=\; d_i \,, \qquad \rho_k \;=\; d_f \,, \tag{45}$$

while the coefficient ρ_1 is used to satisfy interpolation of the initial tangent $\boldsymbol{\rho}'(0)/|\boldsymbol{\rho}'(0)| = \mathbf{t}_i$, decomposed as in (3). Since $\boldsymbol{\rho}'(t) = \rho'(t)\mathbf{o}(t) + \rho(t)\mathbf{o}'(t)$, and $\mathbf{o}'(0) = \mu\mathbf{f}_i$ where μ is positive and specified by (34), we obtain $\boldsymbol{\rho}'(0) = k(\rho_1 - \rho_0)\mathbf{o}_i + \rho_0\mu\mathbf{f}_i$, and one can then verify that the choice

$$\rho_1 \;=\; \rho_0 \left(1 + \frac{\mu s_i}{k c_i} \right) \tag{46}$$

yields $\boldsymbol{\rho}'(0)/|\boldsymbol{\rho}'(0)| = \mathbf{t}_i$. We observe that it is always possible to choose k sufficiently large to ensure that $\rho_1 > 0$. For $k > 2$, the remaining coefficients $\rho_2, \ldots, \rho_{k-1}$ must be chosen to guarantee that $\rho(t) \neq 0$ for $t \in [\,0, 1\,]$. This can be acheieved, for example, through the simple default choice

$$\rho_2 \;=\; \cdots \;=\; \rho_{k-1} \;=\; d_f \,. \tag{47}$$

7 Summary of algorithm

We may summarize the entire procedure as follows.

Algorithm

input: $\mathbf{p}_i = d_i\mathbf{o}_i$, $\mathbf{p}_f = d_f\mathbf{o}_f$, $\mathbf{t}_i$, and $(\mathbf{o}_i, \mathbf{u}_i, \mathbf{v}_i)$, $(\mathbf{o}_f, \mathbf{u}_f, \mathbf{v}_f)$ with $\mathbf{o}_i \neq \mathbf{o}_f$

1. transform the initial data by a spatial rotation that maps $(\mathbf{o}_i, \mathbf{u}_i, \mathbf{v}_i)$ to $(\mathbf{i}, -\mathbf{j}, -\mathbf{k})$;
2. perform the decomposition (3) of $\mathbf{t}_i$, where $c_i > 0$ and the unit vector $\mathbf{f}_i$ is orthogonal to $\mathbf{o}_i$;
3. *end-frame interpolation*: compute interpolants $\mathbf{o}(t)$ on the unit sphere (at most 2) and their associated rational RMDFs $(\mathbf{o}(t), \mathbf{u}(t), \mathbf{v}(t))$ as described in Section 5;

4. compute the positive constant μ defined by expression (34);
5. *end-point & tangent interpolation*: assign $\rho_0, \ldots, \rho_k$ through (45)–(47), $k \geq 2$ being the least integer such that $\rho_1 > 0$, and define $\rho(t)$ by (44);
6. define the interpolant $\boldsymbol{\rho}(t) = \rho(t)\,\mathbf{o}(t)$ and its associated rational RMDF $(\mathbf{o}(t), \mathbf{u}(t), \mathbf{v}(t))$ by (13);
7. transform back to original coordinates by inverting step 1.

output: at most 2 rational curves that satisfy $\boldsymbol{\rho}(t) \neq \mathbf{0}$ for $t \in [\,0, 1\,]$ with rational RMDFs $(\mathbf{o}(t), \mathbf{u}(t), \mathbf{v}(t))$ that interpolate the given data.

8 Numerical experiments

The initial frame $(\mathbf{o}_i, \mathbf{u}_i, \mathbf{v}_i) = (\mathbf{i}, -\mathbf{j}, -\mathbf{k})$ is used in Examples 1–3 below, in keeping with the conventions stated in Section 4. A cubic is required for the polynomial (44) in Example 1, but a quadratic suffices for the other cases. Example 4 illustrates the construction of a G^1 "spline" motion.

Example 1 The data to be interpolated in this case are specified as

$$\mathbf{t}_i = \frac{(-1, -2, 3)}{\sqrt{14}}, \qquad (\mathbf{o}_f, \mathbf{u}_f, \mathbf{v}_f) = (\mathbf{j}, -\mathbf{k}, -\mathbf{i}), \qquad (d_i, d_f) = (3, 2).$$

The unit bisectors of $\mathbf{i}$ with $\mathbf{o}_i$ and $\mathbf{o}_f$ are then $\mathbf{n}_0 = \mathbf{i}$ and $\mathbf{n}_2 = (\mathbf{i} + \mathbf{j})/\sqrt{2}$, and the quantity δ defined by (39) has the value $1/\sqrt{2}$. Hence, the parameter (40) is $\hat{\eta} = \frac{1}{4}\pi$, and $\cos 2\hat{\eta} = 0$. Since, for the given data, we have

$$\mathbf{o}_f \cdot \mathbf{f}_i = -0.554700\,, \quad \mathbf{o}_f \cdot \mathbf{g}_i = -0.832050\,, \quad \mathbf{j}_2 \cdot \mathbf{v}_f = -1\,, \quad \mathbf{k}_2 \cdot \mathbf{v}_f = 0\,,$$

where $\mathbf{j}_2, \mathbf{k}_2$ are defined by (38), the conditions of Proposition 1 are satisfied. The admissible values for the angular variables (ϕ_0, ϕ_1, ϕ_2) are then

$$(0.000000, 0.519146, 3.605240) \quad \text{or} \quad (\pi, 0.519146 + \pi, 3.605240 + \pi)\,,$$

while the parameter μ defined by (29) has the positive value $\mu = 10.301575$. Figure 1 illustrates the steps involved in constructing the motion interpolant.

Example 2 In the second example we consider the data

$$\mathbf{t}_i = \frac{(1, -2, -3)}{\sqrt{14}}, \quad \mathbf{o}_f = \frac{(-1, -2, -4)}{\sqrt{21}}, \quad \mathbf{u}_f = \mathbf{j}_2\,, \quad \mathbf{v}_f = \mathbf{k}_2\,,$$

where $\mathbf{j}_2, \mathbf{k}_2$ are defined by (38), and $(d_i, d_f) = (1.5, 2.0)$. In this case

$$\mathbf{o}_f \cdot \mathbf{f}_i = 0.968364\,, \quad \mathbf{o}_f \cdot \mathbf{g}_i = 0.121046\,, \quad \mathbf{j}_2 \cdot \mathbf{v}_f = 0\,, \quad \mathbf{k}_2 \cdot \mathbf{v}_f = 1\,,$$

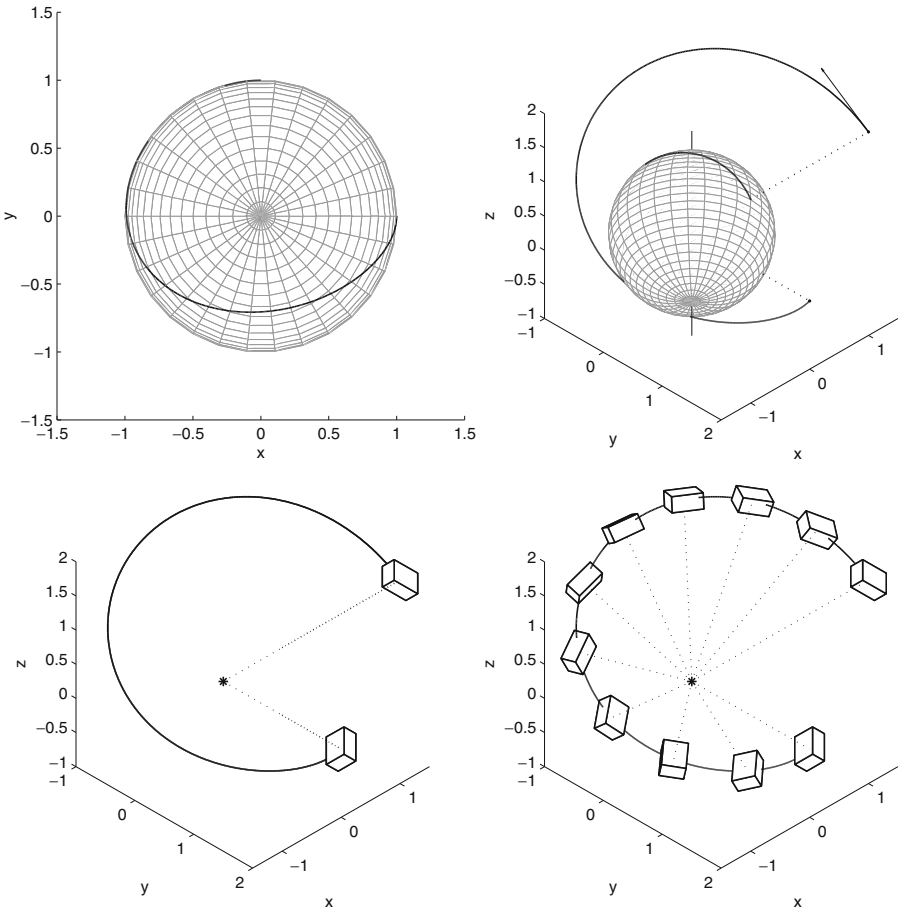

Fig. 1 Construction of the interpolant in Example 1. *Top left* The polar indicatrix $\mathbf{o}(t) = \mathbf{r}(t)/|\mathbf{r}(t)|$ on the unit sphere, obtained from a P quartic $\mathbf{r}(t)$ with a rational RMDF that interpolates the data (5)–(7). *Top right* The rational space curve $\boldsymbol{\rho}(t) = \rho(t)\mathbf{o}(t)$ with a rational RMDF interpolating the data (1)–(2), obtained by scaling $\mathbf{o}(t)$ by the polynomial (44). *Bottom left* The camera path together with the initial and final camera orientations. *Bottom right* Sampling of the camera motion along the constructed path, with orientation specified by the rational RMDF along $\boldsymbol{\rho}(t)$

so Proposition 1 is again satisfied. The admissible (ϕ_0, ϕ_1, ϕ_2) values are

$$(0.000000, 0.124355, 0.000000) \quad \text{or} \quad (\pi, 0.124355 + \pi, \pi)\,,$$

and (29) is satisfied with $\mu = 1.935815$. The interpolant is shown in Fig. 2.

Example 3 For this example, we use the initial tangent vector

$$\mathbf{t}_i = \frac{(1, -2, -3)}{\sqrt{14}}\,,$$

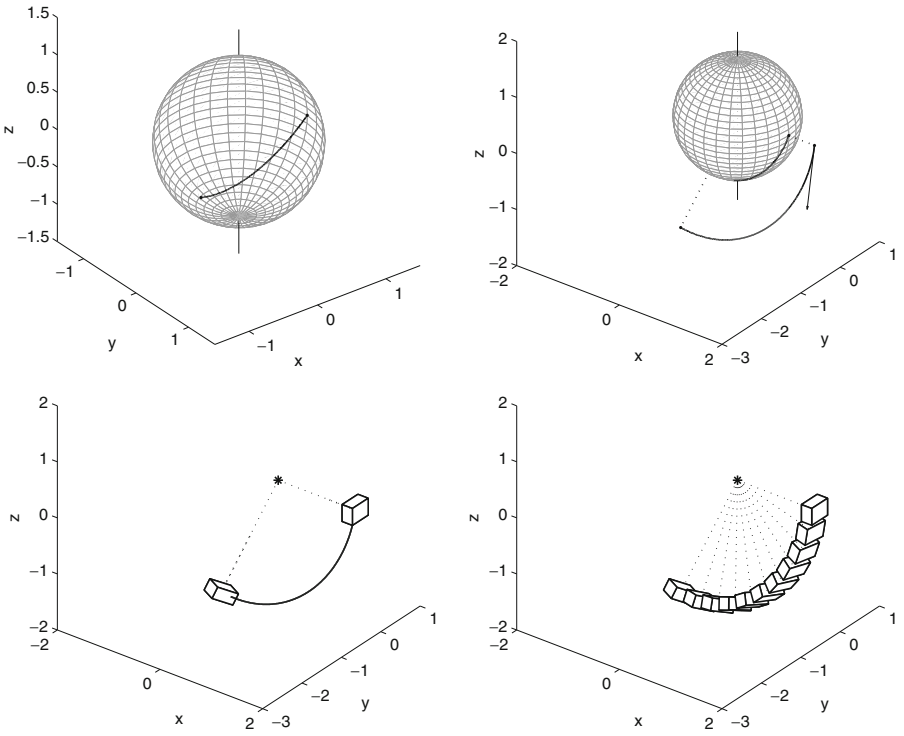

Fig. 2 The interpolant in Example 2. *Top left* The polar indicatrix $\mathbf{o}(t)$ on the unit sphere. *Top right* The rational space curve $\boldsymbol{\rho}(t) = \rho(t)\mathbf{o}(t)$ with a rational RMDF that interpolates the data (1)–(2). *Bottom left* The camera path, with initial and final camera orientations. *Bottom right* Sampling of the camera motion, with orientation specified by the rational RMDF on $\boldsymbol{\rho}(t)$

the final frame specified by

$$\mathbf{o}_f = (-0.963624, -0.148250, -0.222375)\,,$$
$$\mathbf{u}_f = (-0.152057, 0.988372, 0.000000)\,,$$
$$\mathbf{v}_f = (0.219789, 0.033814, -0.974961)\,,$$

and the polar distances $(d_i, d_f) = (1.5, 2.0)$. In this case $\mathbf{o}_f \cdot \mathbf{g}_i = 0$, and one can verify that $\delta = 0.134863$ and $\hat{\eta} = 1.435521$ radians. Hence, the conditions of Proposition 3 (see the Appendix) are satisfied, and the admissible values for (ϕ_0, ϕ_1, ϕ_2) are

$$(0.000000, 5.188873, 1.094313) \quad \text{or} \quad (\pi, 5.188873 + \pi, 1.094313 + \pi)\,.$$

Correspondingly (29) is satisfied with $\mu = 8.193661$. Figure 3 illustrates the resulting camera motion. Note that, in this case, the polar indicatrix $\mathbf{o}(t)$ is not a great circle arc on the unit sphere, even though the end points $\mathbf{o}_i, \mathbf{o}_f$ and

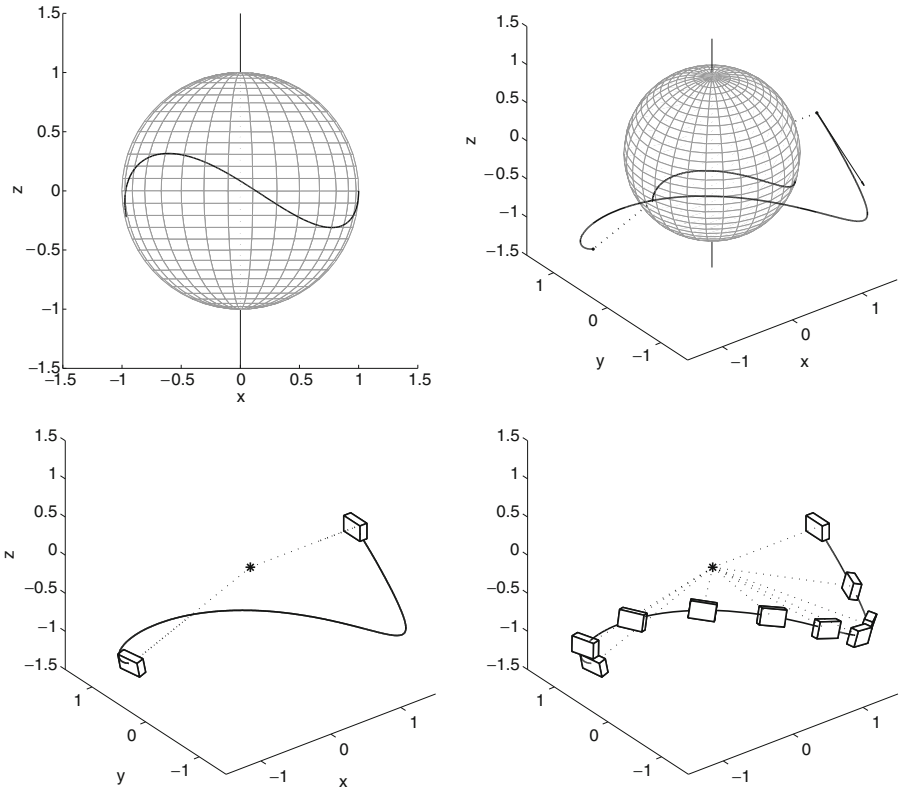

Fig. 3 Construction of camera motion in Example 3. *Top left* The polar indicatrix $\mathbf{o}(t)$ on the unit sphere. *Top right* Corresponding rational curve $\boldsymbol{\rho}(t) = \rho(t)\mathbf{o}(t)$ with a rational RMDF, that interpolates the data (1)–(2). *Bottom left* The curve $\boldsymbol{\rho}(t)$ shown with initial and final camera orientations. *Bottom right* Sampling of the camera motion along the constructed path, with orientation specified by the rational RMDF along $\boldsymbol{\rho}(t)$

initial tangent $\mathbf{f}_i$ are coplanar, because the great circle arc does not admit a rational RMDF interpolating the prescribed end frames.

Compared with Examples 1 and 2, the camera path in this example seems rather more convoluted, although its orientation is rotation-minimizing. In order to secure the rotation-minimizing property with residual freedoms that can be used to optimize the path geometry, it is necessary to use interpolants of higher order than the minimal-degree solutions adopted herein.

Example 4 The final example is concerned with construction of a "spline" motion by interpolating discrete data sampled from the circular helix $\mathbf{r}(t) = (r\cos\theta, r\sin\theta, k\theta)$ with $r = 2$, $k = 1$. Four equidistant points on the intervals $\theta \in [\,0, \frac{1}{2}\pi\,]$, $\theta \in [\,0, \pi\,]$, and $\theta \in [\,0, 2\pi\,]$ were used. The segment end points are defined by the sample points on the helix, and the initial tangent for the first segment coincides with that of the helix. To obtain a G^1 motion, the initial

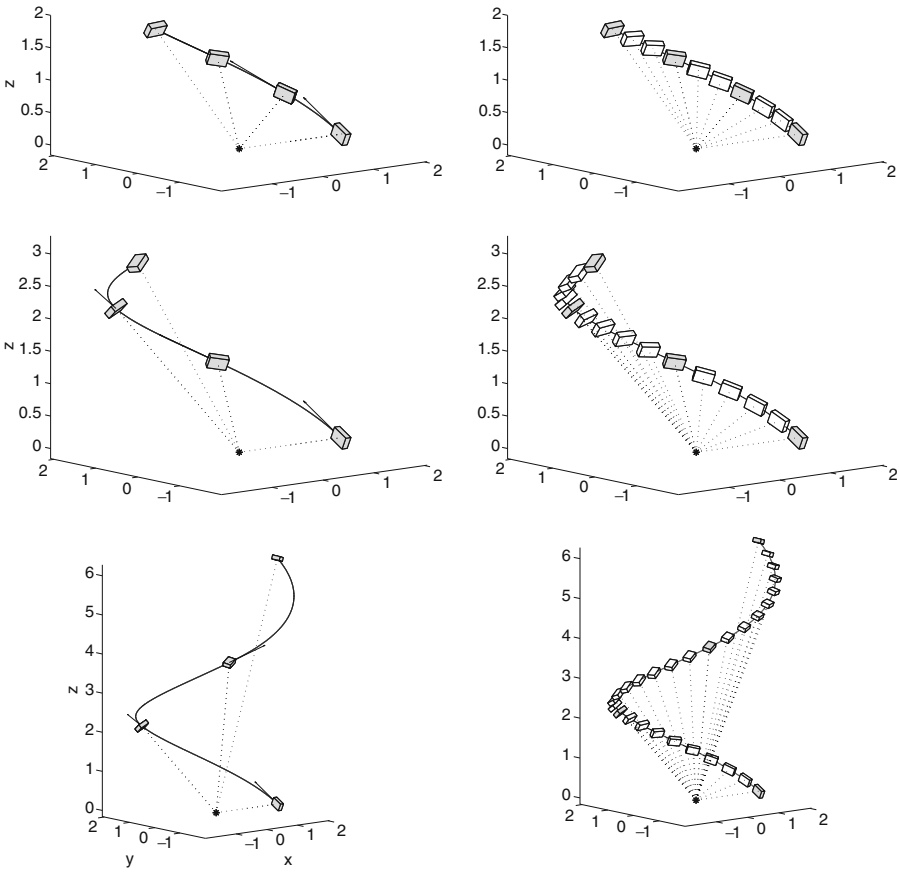

Fig. 4 G^1 rational RMDF motion interpolants to data sampled at $\theta = 0, \pi/6, \pi/3, \pi/2$ (*top*), $\theta = 0$, $\pi/3$, $2\pi/3$, π (*middle*), and $\theta = 0$, $2\pi/3$, $4\pi/3$, 2π (*bottom*) from the circular helix in Example 4. The discrete data defining the motion interpolants is shown on the *left*, and the corresponding variation of camera orientation is indicated by a rectangular parallelepiped on the *right*

tangent for each subsequent segment coincides with the final tangent of the preceding segment. The frame orientations at the sample points are defined by the known (exact) variation of the RMDF on a circular helix: see Example 2 in [7]. Figure 4 illustrates the resulting G^1 motion interpolants.

9 Closure

A scheme for the design of rational rotation-minimizing camera motions, that guarantees the least apparent rotation of the object being imaged, has been developed. The method is based on translating the known characterization of rational rotation-minimizing *adapted* frames on space curves to the context of

directed frames (incorporating the unit polar vector, rather than the tangent, as a reference for the frame angular velocity). A motion segment is defined by initial/final camera positions, orientations, and an initial motion direction.

In principle, such segments may be splined together to yield G^1 motions interpolating a sequence of camera positions/orientations. However, as with the lowest-order "ordinary" splines (namely, C^1 quadratics) that interpolate position data only, the resulting motion interpolants may not be sufficiently smooth for some applications. The interpolation of position/orientation data by higher-order curves with rational RMDFs, that provide a greater degree of shape flexibility, is therefore of considerable interest.

The procedure described herein is based on using the lowest-degree curves with sufficient freedoms to interpolate the prescribed data, and conditions for the existence of solutions have been determined. Using curves of higher order should help to ensure existence of interpolants to arbitrary data, and provide residual freedoms for optimization purposes. This requires characterizations for rational RMDFs on higher-order curves than the P quartics.

Acknowledgements The second author was partially supported through the Young Researchers Program in the Gruppo Nazionale per il Calcolo Scientifico (GNCS) of the Istituto Nazionale di Alta Matematica Francesco Severi (INdAM).

Appendix

We now prove Proposition 1 in Section 4, which states sufficient conditions on the end frame orientations to ensure that one of the two admissible values β_A, β_B for the difference $\phi_2 - \phi_0$ satisfies the inequality (35).

To clarify how these conditions arise, we recall the two-step procedure used in [10] to compute β so as to ensure interpolation of the end frames (see [10] for complete details). In the first step, the angle ϕ_0 and another angle η are determined from the relations

$$(\sin 2\phi_0, \cos 2\phi_0) \;=\; (-\mathbf{j}_0 \cdot \mathbf{v}_i, \mathbf{k}_0 \cdot \mathbf{v}_i)\,, \tag{48}$$

$$(\sin 2\eta, \cos 2\eta) \;=\; (-\mathbf{j}_2 \cdot \mathbf{v}_f, \mathbf{k}_2 \cdot \mathbf{v}_f)\,, \tag{49}$$

the vectors $\mathbf{j}_0, \mathbf{j}_2$ and $\mathbf{k}_0, \mathbf{k}_2$ being defined by (38). Note that for $(\mathbf{o}_i, \mathbf{u}_i, \mathbf{v}_i) = (\mathbf{i}, -\mathbf{j}, -\mathbf{k})$ we have $\mathbf{n}_0 = \mathbf{i}$, and hence $(\mathbf{j}_0, \mathbf{k}_0) = (-\mathbf{j}, -\mathbf{k})$, $(\mathbf{u}_i, \mathbf{v}_i) = (\mathbf{j}_0, \mathbf{k}_0)$ and $\phi_0 = 0$ or π. For the other angle η there are also two possibilities—$\eta_A \in [\,0, \pi)$ and $\eta_B \in [\,-\pi, 0)$, with $\eta_B = \eta_A - \pi$.

In the second step $\beta = \phi_2 - \phi_0$ is determined by requiring [10] that

$$\arg\left(\sqrt{1 - (\gamma\cos\beta + \delta\sin\beta)^2}\,\boldsymbol{\zeta}_0 \;-\; \cos\beta\,\boldsymbol{\zeta}_1 \;-\; \sin\beta\,\boldsymbol{\zeta}_2\right) \;=\; \phi_0 - \eta\,, \tag{50}$$

where $\gamma = \mathbf{i} \cdot (\mathbf{n}_2 \times \mathbf{n}_0)$, δ is defined by (39), and we set

$$\boldsymbol{\zeta}_0 \;=\; \delta + \mathrm{i}\,\gamma\,, \qquad \boldsymbol{\zeta}_1 \;=\; \gamma^2 - 1 - \mathrm{i}\,\gamma\delta\,, \qquad \boldsymbol{\zeta}_2 \;=\; \gamma\delta + \mathrm{i}\,(1 - \delta^2)\,.$$

In the present context, $\mathbf{n}_0 = \mathbf{i}$ implies that $\gamma = 0$, and we can assume $\phi_0 = 0$ without loss of generality (as noted in Section 4), so (50) becomes

$$\arg\left(\delta\sqrt{1-\delta^2\sin^2\beta} + \cos\beta + \mathrm{i}\,(1-\delta^2)\sin\beta\right) = \eta\,, \tag{51}$$

where $\eta = \eta_A$ or η_B. Now as β varies from $-\pi$ to $+\pi$, the complex value whose argument appears on the left in (51) executes a closed path in the complex plane that encircles the origin when $|\delta| < 1$—which holds here since $\mathbf{n}_0 = \mathbf{i}$, (19), and (39) imply that $0 \le \delta < 1$ when $\mathbf{o}_f \neq \mathbf{o}_i$. Consequently, (51) admits a unique solution for each value of the angle η on the right, and we shall henceforth denote by $\beta_A \in [\,0, \pi\,)$ and $\beta_B \in [-\pi, 0)$ the solutions associated with η_A and η_B, respectively.

We now prove Proposition 1, stating sufficient conditions on the data to guarantee the existence of exactly one rational curve with a rational RMDF interpolating the end-points, end-frames, and the initial tangent (1)–(2). In particular we show that, for the given data, exactly one of β_A, β_B satisfies (35). Proposition 1 addresses the generic case with $\mathbf{o}_f \cdot \mathbf{f}_i \neq 0$ and $\mathbf{o}_f \cdot \mathbf{g}_i \neq 0$, while the special cases $\mathbf{o}_f \cdot \mathbf{g}_i = 0$ and $\mathbf{o}_f \cdot \mathbf{f}_i = 0$ are treated in Propositions 3 and 4 below. It is convenient to express these results in terms of the angle $\hat{\eta} \in (0, \frac{1}{2}\pi\,]$ defined by (40), equal to the right-hand side of (51) when $\beta = \frac{1}{2}\pi$. Note that, when $\beta = -\frac{1}{2}\pi$, the angle on the right in (51) is equal to $-\hat{\eta}$.

Proof of Proposition 1 Consider first the case $\mathbf{o}_f \cdot \mathbf{f}_i > 0$ and $\mathbf{o}_f \cdot \mathbf{g}_i > 0$. Then the angle (36) satisfies $\beta^* \in \left(0, \frac{1}{2}\pi\right)$, and the inequality (35) holds if and only if β lies in the interval $(-\beta_*, \pi - \beta_*)$ specified in (37). Hence $\left[\,0, \frac{1}{2}\pi\,\right] \subset (-\beta_*, \pi - \beta_*)$ and $\left[\,-\pi, -\frac{1}{2}\pi\,\right] \cap (-\beta_*, \pi - \beta_*) = \emptyset$. So it suffices to show that the conditions (41) imply that $\beta_A \in \left[\,0, \frac{1}{2}\pi\,\right]$ and $\beta_B \in [\,-\pi, -\frac{1}{2}\pi\,]$. Now from the definition (49) of η, the conditions (41) allow us to conclude that $\eta_A \in [\,0, \hat{\eta}\,]$ and $\eta_B \in [\,-\pi, -\pi + \hat{\eta}\,] \subseteq [\,-\pi, -\hat{\eta}\,]$. Thus, it follows also that $\beta_A \in [\,0, \frac{1}{2}\pi\,]$ and $\beta_B \in \left[\,-\pi, -\frac{1}{2}\pi\,\right]$. The proofs for the other three possibilities, depending on the signs of $\mathbf{o}_f \cdot \mathbf{f}_i$ and $\mathbf{o}_f \cdot \mathbf{g}_i$, are analogous. □

Proposition 3 *If $\mathbf{o}_f \cdot \mathbf{g}_i = 0$ and $\hat{\eta}$ is defined by (40), exactly one of the two values β_A, β_B satisfies (35) when*

$$\mathbf{k}_2 \cdot \mathbf{v}_f \;>\; \cos 2\hat{\eta}\,. \tag{52}$$

Proof Consider the case $\mathbf{o}_f \cdot \mathbf{f}_i > 0$. Then the angle (36) is $\beta^* = \frac{1}{2}\pi$, and $(-\beta^*, \pi - \beta^*) = \left(-\frac{1}{2}\pi, \frac{1}{2}\pi\right)$. Now from (49) and (52) we must have $\eta_A \in [\,0, \hat{\eta})$ or $\eta_A \in (\pi - \hat{\eta}, \pi\,]$. If $\eta_A \in [\,0, \hat{\eta})$ then $\eta_B \in \left[\,-\pi, -\pi + \hat{\eta}\right) \subseteq [\,-\pi, -\hat{\eta})$, so $\beta_A \in [\,0, \frac{1}{2}\pi)$ and $\beta_B \in \left[\,-\pi, -\frac{1}{2}\pi\right)$. Then β_A is admissible and β_B is not. By analogous arguments one can verify that, if $\eta_A \in (\pi - \hat{\eta}, \pi\,]$, then β_B is admissible and β_A is not. The proof for the case $\mathbf{o}_f \cdot \mathbf{f}_i < 0$ is similar. □

The last result addresses the case $\mathbf{o}_f \cdot \mathbf{f}_i = 0$, and shows that the method always produces one interpolant—except when $\mathbf{v}_f = \mathbf{k}_2$ (the inequality (31)

cannot hold in this case, since $\mathbf{v}_f = \mathbf{k}_2$ implies that $\eta_A = 0$ and $\eta_B = -\pi$, and consequently $\beta_A = 0$ and $\beta_B = -\pi$).

Proposition 4 *If* $\mathbf{o}_f \cdot \mathbf{f}_i = 0$ *and* $\mathbf{v}_f \neq \mathbf{k}_2$, *exactly one of the two values* β_A, β_B *satisfies* (35).

Proof In this case, the angle (36) is $\beta^* = 0$ when $\mathbf{o}_f \cdot \mathbf{g}_i > 0$, and $\beta_* = \pi$ when $\mathbf{o}_f \cdot \mathbf{g}_i < 0$. Now in general, $\beta_A \in [0, \pi)$ and $\beta_B \in [-\pi, 0)$. However, since $\mathbf{v}_f \neq \mathbf{k}_2$, we have $\eta_A \neq 0$ and $\eta_B \neq -\pi$, which imply that $\beta_A \in (0, \pi)$ and $\beta_B \in (-\pi, 0)$. Thus, exactly one of them belongs to the interval (37) identifying the angles β that satisfy (35). □

References

1. Barton, M., Jüttler, B., Wang, W.: Construction of rational curves with rational rotation-minimizing frames via Möbius transformations. In: Dæhlen, M., et al. (eds.) MMCS 2008. Lecture Notes in Computer Science 5862, pp. 15–25. Springer, Berlin (2010)
2. Choi, H.I., Han, C.Y.: Euler–Rodrigues frames on spatial Pythagorean–hodograph curves. Comput. Aided Geom. Des. **19**, 603–620 (2002)
3. Choi, H.I., Lee, D.S., Moon, H.P.: Clifford algebra, spin representation, and rational parameterization of curves and surfaces. Adv. Comput. Math. **17**, 5–48 (2002)
4. Christie, M., Machap, R., Normad, J.-M., Oliver, P., Pickering, J.: Virtual camera planning: a survey. In: Butz, A., et al. (eds.) Proceedings of Smart Graphics 2005. Lecture Notes in Computer Science 3638, pp. 40–52. Springer, Berlin (2005)
5. Farouki, R.T.: Pythagorean-Hodograph Curves: Algebra and Geometry Inseparable. Springer, Berlin (2008)
6. Farouki, R.T.: Quaternion and Hopf map characterizations for the existence of rational rotation-minimizing frames on quintic space curves. Adv. Comput. Math. **33**, 331–348 (2010)
7. Farouki, R.T., Giannelli, C.: Spatial camera orientation control by rotation-minimizing directed frames. Comput. Anim. Virtual World **20**, 457–472 (2009)
8. Farouki, R.T., Giannelli, C., Manni, C., Sestini, A.: Identification of spatial PH quintic Hermite interpolants with near-optimal shape measures. Comput. Aided Geom. Des. **25**, 274–297 (2008)
9. Farouki, R.T., Giannelli, C., Manni, C., Sestini, A.: Quintic space curves with rational rotation-minimizing frames. Comput. Aided Geom. Des. **26**, 580–592 (2009)
10. Farouki, R.T., Giannelli, C., Manni, C., Sestini, A.: Design of rational rotation-minimizing rigid body motions by Hermite interpolation. Math. Comput. (2011). doi:10.1090/S0025-5718-2011-02519-6
11. Farouki, R.T., Sakkalis, T.: Rational rotation-minimizing frames on polynomial space curves of arbitrary degree. J. Symb. Comput. **45**, 844–856 (2010)
12. Farouki, R.T., Sir, Z.: Rational Pythagorean–hodograph space curves. Comput. Aided Geom. Des. **28**, 75–88 (2011)
13. Han, C.Y.: Nonexistence of rational rotation-minimizing frames on cubic curves. Comput. Aided Geom. Des. **25**, 298–304 (2008)
14. Nieuwenhuisen, D., Overmars, M.H.: Motion planning for camera movements. In: Proceedings, IEEE International Conference on Robotics & Automation, New Orleans, LA, pp. 3870–3876 (2004)